

Ultrasound Image Enhancement Using Laplacian Kernel Set

Mohit Samnotra¹, Akshay Girdhar²

Dept. of CSE, Guru Nanak Dev Engineering College, Ludhiana, India^{1,2}

Abstract: Biomedical imaging methods are very vital for health care services. The random noise in the biomedical images may cause critical damage to the patient. The aim of this thesis was to investigate the advanced restoration and enhancement filters, identify their merits and demerits and propose new filters to overcome the drawbacks of the existing filters. For this purpose kernel set based filters were applied to normal ultrasound image. The performance parameters such as signal to noise ratio (SNR), peak signal to noise ratio (PSNR), root mean square error (RMSE), mean absolute error (MAE), and Pearson correlation coefficient (PCC) have been estimated and compared.

Keywords: Ultrasound, Kernel set, Laplacian, SNR, PSNR.

I. INTRODUCTION

Medical imaging has become increasingly important in bio-medical research and clinical practice. It is the driving force in the development of modern volumetric digital imaging techniques [1-2]. In medical clinical research and practice, imaging has become an essential part to diagnose and to study anatomy and function of the human body. Some of the imaging techniques that noninvasively can reveal tumors and fractures with a minimal hazard to the living tissue are MRI, X-ray, and ultrasound. A kidney stone is a hard, crystalline mineral material formed within the kidney or urinary tract. Kidney stones are a common cause of blood in the urine and often severe pain in the abdomen, flank, or groin. Kidney stones are sometimes called renal calculi. Ultrasound has been used to image the human body for over half a century. Dr. Karl Theo Dussik, an Austrian neurologist, was the first to apply ultrasound as a medical diagnostic tool to image the brain [3-4]. Today, ultrasound is one of the most widely used imaging technologies in medicine. It is portable, free of radiation risk, and relatively inexpensive when compared with other imaging modalities, such as magnetic resonance and computed tomography. Furthermore, ultrasound images are tomographic, i.e., offering a “cross-sectional” view of anatomical structures. The images can be acquired in “real time,” thus providing instantaneous visual guidance for many interventional procedures including those for regional anesthesia and pain management.

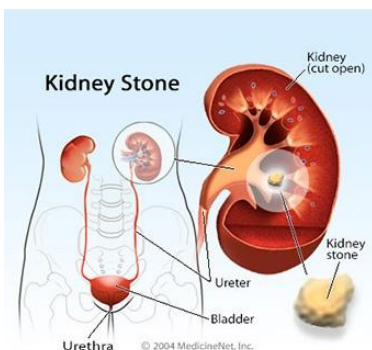


Fig. 1 Anatomy of human kidney.

Modern medical ultrasound is performed primarily using a pulse-echo approach with a brightness mode (B-mode) display. The basic principles of B-mode imaging are much the same today as they were several decades ago. This involves transmitting small pulses of ultrasound echo from a transducer into the body. As the ultrasound waves penetrate body tissues of different acoustic impedances along the path of transmission, some are reflected back to the transducer (echo signals) and some continue to penetrate deeper. The echo signals returned from many sequential coplanar pulses are processed and combined to generate an image [5-8].

II. LAPLACIAN FILTER

An. Linear features in an image are identified using the contrast between the pixels on either side of it. Contrast between the pixels varies with the difference in the pixel values between them. A first order derivative simply shows the difference in the pixel value for adjacent pixels. On the other hand, second order derivative shows the difference in the first derivative and is better capable of identifying the thin linear features and noises in the image. It also gives very high values for the pixels corresponding to the noises in the data. Laplacian filter is a non-directional filter based on the second spatial derivative of the pixel values [9]. The second order derivative in the x and y direction may be represented as given in Fig. 2.

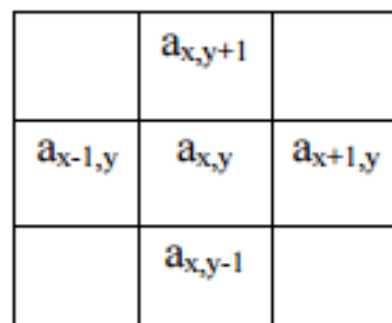


Fig. 2 Schematic of the Laplacian filter kernel.

$$\frac{\partial^2 a}{\partial^2 x^2} = a_{x-1} + a_{x+1} - 2a_x$$

$$\frac{\partial^2 a}{\partial^2 y^2} = a_{y-1} + a_{y+1} - 2a_y$$

$$\begin{aligned} \nabla^2 a &= \frac{\partial^2 a}{\partial^2 x^2} + \frac{\partial^2 a}{\partial^2 y^2} \\ &= a_{x-1} + a_{x+1} + a_{y-1} + a_{y+1} - 4a_{x,y} \end{aligned}$$

This equation is implemented using a kernel with -4 at the center, and 1 at the 4 adjacent directions as shown in Fig. 3.

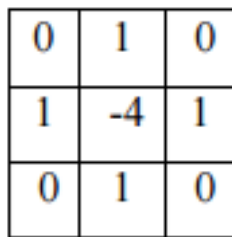


Fig. 3.Laplace filter kernel.

The Laplacian filters are considered to be highly effective in detecting the edges irrespective of the orientation of the lineament. During edge enhancement using Laplacian filter, the kernel is placed over 3x3 array of original pixels and each pixel is multiplied by the corresponding value in the kernel. The nine resulting values are summed and resultant kernel value is combined with the central pixel of 3x3 array. Laplacian filter will enhance edges in all the directions excepting those in the direction of the movement of the filter (i.e., linear features with east-west orientation will not get enhanced) [10-12].

III.METHODOLOGY

The research work is carried to enhance ultrasound image using Laplacian kernels set technique. In order to proceed with the research work image processing toolbox is used. The work is divided into two major parts. The main goal of image enhancement is to reduce redundancy in the image as much as possible. Figures 4 shows the ultrasound image used in the research work. Kernel set method is one of simple and easy to implement image sharpening algorithms.

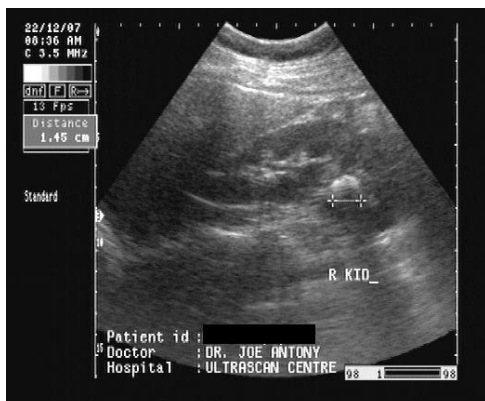


Fig. 4 Ultrasound image kidney with stone.

The designed algorithm to enhance the image employing kernel set is shown in Fig. 5.

The image is converted into double data type and then multi dimensional filter is applied on the input image.

Two different boundary conditions are taken for the filtering process i.e. symmetric (input array values outside the bounds of the array are computed by mirror-reflecting the array across the array border) and replicate (input array values outside the bounds of the array are assumed to equal the nearest array border value).

$$\begin{bmatrix} 0 & -1 & 0 \\ 0 & 3 & 0 \\ 0 & -1 & 0 \end{bmatrix} \quad \begin{bmatrix} -1 & 0 & -1 \\ 0 & 5 & 0 \\ -1 & 0 & -1 \end{bmatrix} \quad \begin{bmatrix} -1 & 2 & -1 \\ 0 & 1 & 0 \\ -1 & 2 & -1 \end{bmatrix}$$

$$K = 1 \quad K = 2 \quad K = 3$$

$$\begin{bmatrix} -1 & 0 & -1 \\ 2 & 1 & 2 \\ -1 & 0 & -1 \end{bmatrix} \quad \begin{bmatrix} -1 & 0 & -1 \\ -1 & 7 & -1 \\ -1 & 0 & -1 \end{bmatrix} \quad \begin{bmatrix} -1 & -1 & -1 \\ 0 & 7 & 0 \\ -1 & -1 & -1 \end{bmatrix}$$

$$K = 4 \quad K = 5 \quad K = 6$$

$$\begin{bmatrix} -1 & -1 & -1 \\ 1 & 5 & 1 \\ -1 & -1 & -1 \end{bmatrix} \quad \begin{bmatrix} -1 & 1 & -1 \\ 0 & 3 & 0 \\ -1 & 1 & -1 \end{bmatrix} \quad \begin{bmatrix} 0 & -2 & 0 \\ 0 & 5 & 0 \\ 0 & -2 & 0 \end{bmatrix}$$

$$K = 7 \quad K = 8 \quad K = 9$$

$$\begin{bmatrix} -2 & 0 & -2 \\ 0 & 9 & 0 \\ -2 & 0 & -2 \end{bmatrix} \quad \begin{bmatrix} 0 & -1 & 0 \\ -1 & 5 & -1 \\ 0 & -1 & 0 \end{bmatrix} \quad \begin{bmatrix} -1 & 0 & -1 \\ -2 & 9 & -2 \\ -1 & 0 & -1 \end{bmatrix}$$

$$K = 10 \quad K = 11 \quad K = 12$$

$$\begin{bmatrix} -2 & -1 & -2 \\ 0 & 11 & 0 \\ -2 & -1 & -2 \end{bmatrix} \quad \begin{bmatrix} -1 & -2 & -1 \\ 0 & 11 & 0 \\ -1 & -2 & -1 \end{bmatrix} \quad \begin{bmatrix} -1 & -2 & -1 \\ -1 & 11 & -1 \\ -1 & -2 & -1 \end{bmatrix}$$

$$K = 13 \quad K = 14 \quad K = 15$$

$$\begin{bmatrix} 0 & -2 & 0 \\ -1 & 7 & -1 \\ 0 & -2 & 0 \end{bmatrix} \quad \begin{bmatrix} 0 & 0 & 0 \\ -1 & 3 & -1 \\ 0 & 0 & 0 \end{bmatrix} \quad \begin{bmatrix} -2 & 0 & -2 \\ -1 & 11 & -1 \\ -2 & 0 & -2 \end{bmatrix}$$

$$K = 16 \quad K = 17 \quad K = 18$$

$$\begin{bmatrix} 0 & -1 & 0 \\ -2 & 7 & -2 \\ 0 & -1 & 0 \end{bmatrix} \quad \begin{bmatrix} -2 & 0 & -2 \\ 1 & 7 & 1 \\ -2 & 0 & -2 \end{bmatrix}$$

$$K = 19 \quad K = 20$$

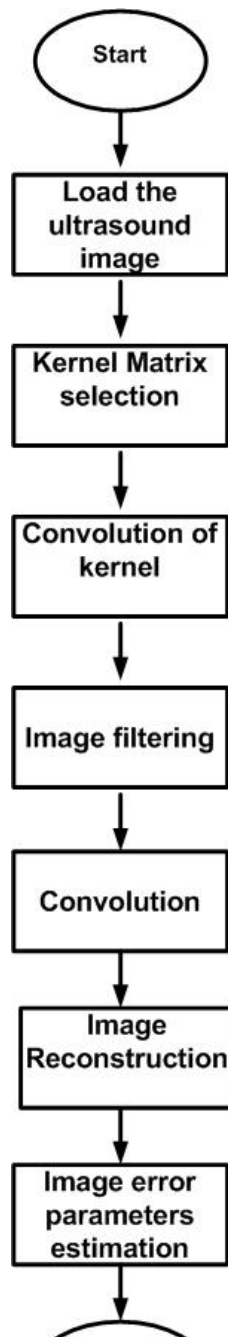


Fig. 5 Ultrasound image kidney with stone.

In second part various image characteristic parameters such as signal to noise ratio (SNR), peak signal to noise ratio (PSNR), root mean square error (RMSE), Pearson correlation coefficient (PCC), and mean absolute error (MAE) are estimated for compressed image with respect to original image.

IV. RESULTS AND DISCUSSION

Results obtained by convolution of twenty kernel matrices with normal ultra sound image of kidney having stone in it are presented in this section. It is observed from the reconstructed image that the entire kernel matrix does not provide enhanced image. The reconstructed image from K1, K3, K8, K9, K11, K16, and K17 are having good quality as compared to other kernel matrix.

TABLE I .COMPUTED VALUES OF SNR AND PSNR RECONSTRUCTED FILTERED IMAGE

Kernel Matrix	SNR (dB)	PSNR (dB)
K1	0.14	23.52
K2	0.43	18.72
K3	0.24	21.6
K4	0.23	19.87
K5	0.51	17.72
K6	0.55	16.86
K7	0.48	17.47
K8	0.32	21.09
K9	0.29	19.21
K10	0.75	15.17
K11	0.29	21.22
K12	0.58	16.82
K13	0.85	14.28
K14	0.67	15.49
K15	0.74	15.05
K16	0.41	18.36
K17	0.17	24.98
K18	0.81	14.73
K19	0.38	19.41
K20	0.69	15.62

TABLE II .COMPUTED VALUES OF SNR AND PSNR RECONSTRUCTED FILTERED IMAGE

Kernel Matrix	RMSE	MAE	PCC
K1	108.92	12.88	646987.9
K2	169.43	24.74	603750.0
K3	100.34	13.92	630344.7
K4	149.08	19.95	613314.8
K5	178.86	27.65	588053.0
K6	185.22	30.79	573777.8
K7	178.29	28.58	584220.9
K8	137.11	17.79	630191.3
K9	154.29	22.02	606504.5
K10	201.96	37.13	539283.3
K11	136.79	17.75	631241.4
K12	186.66	30.32	571554.0
K13	207.19	40.51	518792.5
K14	194.61	35.55	546338.3
K15	199.58	37.21	536396.3
K16	168.08	25.21	597427.2
K17	69.57	9.67	654289.1
K18	206.09	38.68	528664.3
K19	155.24	21.93	611113.8
K20	197.81	35.61	549366.9

The image characteristics parameters such as signal to noise ratio (SNR), peak signal to noise ratio (PSNR), mean absolute error (MAE), root mean square error (RMSE), and Pearson correlation coefficient (PCC) for are the reconstructed image with kernel matrices are computed and tabulate in Table I and Table II. The maximum and minimum SNR values comes out to be 0.85 dB (K13) and 0.17 dB (K17). 24.28 dB and 14.28 dB are the maximum

and minimum PSNR values. MAE comes out to be 207.19 and 69.57 maximum and minimum value respectively. Similarly, RMSE have maximum value of 40.51 and minimum value of 9.67. PCC have maximum value of 65.42×10^4 and minimum value of 51.87×10^4 . Figure 6 shows the graphical representation of computed SNR values for all the kernel matrices. The PSNR is shown in Fig. 7 and RMSE is shown in Fig. 8. In the graph x-axis represents the kernel matrix and y-axis the magnitude.

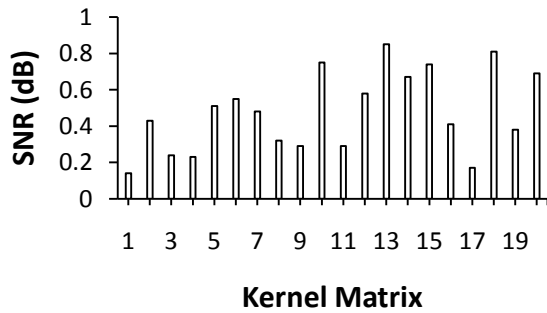


Fig.6 Computed SNR for normal US image.

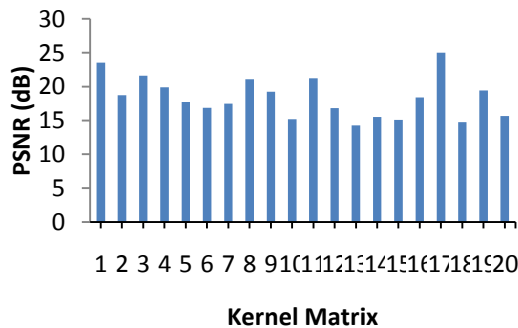


Fig. 7 Computed PSNR for normal US image.

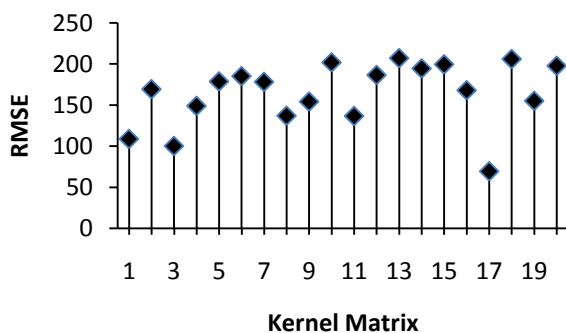


Fig. 8 Computed RMSE for normal US image.

V. CONCLUSION

Research work is carried out to enhance the ultrasound image of kidney containing stone with digital image processing technique. Four sets of experiments were carried out with twenty set of kernel matrices. A normal ultrasound image subjected to the filter designed using kernel set. It is observed that all the kernel set does not enhance the image but some degrades the image also. The computed image characteristics parameters for images

convoluted with kernel matrices which information regarding the image are K1 (SNR = 0.14 dB, PSNR = 23.52 dB, RMSE = 108.92, MAE = 12.88), K3 (SNR = 0.24 dB, PSNR = 21.6 dB, RMSE = 100.34, MAE = 13.92), K8 (SNR = 0.32 dB, PSNR = 21.09 dB, RMSE = 137.11, MAE = 17.79), K9(SNR = 0.29 dB, PSNR = 19.21 dB, RMSE = 154.29, MAE = 22.02), K11(SNR = 0.29 dB, PSNR = 21.22 dB, RMSE = 136.79, MAE = 17.75), K16 (SNR = 0.41 dB, PSNR = 18.36 dB, RMSE = 168.08, MAE = 25.21), K17 (SNR = 0.17 dB, PSNR = 24.98 dB, RMSE = 69.57, MAE = 9.67).

REFERENCES

- [1] S. K. Jespersen, J. E. Wilhjelm, and H. Sillesen, "Multi-Angle Compound Imaging," *Ultrasonic Imaging*, vol. 20, no. 2, pp. 81–102, Apr. 1998.
- [2] D. Palumbo, B. Yee, P. O’Dea, S. Leedy, S. Viswanath and A. Madabhushi, Editors, "Interplay between Bias Field Correction, Intensity Standardization, and Noise Filtering for T2-weighted MRI", *Annual International Conference of the IEEE Engineering in Medicine and Biology Society (EMBC)*, Boston, MA, USA, 2011.
- [3] X. Yan, M. Zhou, L. Xu, W. Liu and G. Yang, Editors, "Noise Removal of MRI data with Edge Enhancing", *5th International Conference on Bioinformatics and Biomedical Engineering (ICBBE)*, Wuhan, China, 2011.
- [4] A. K. Hmood, Z. M. Kasirun, H. A. Jalab, G. M. Alam, A. A. Zaidan and B. B. Zaidan, "On the accuracy of hiding information metrics: Counterfeit protection for education and important certificates", *International Journal of the Physical Sciences*, vol. 5, pp. 1054-1062, 2010.
- [5] Ashish Khare, Uma Shanker Tiwary, Moongu Jeon, "Daubechies complex wavelet transform based multilevel shrinkage for deblurring of medical images in presence of noise," *International Journal of Wavelets, Multiresolution and Information Processing*, Vol. 7, pp. 587-604, 2009.
- [6] S. Setzer, G. Steidl, T. Teuber, "Deblurring Poissonian images by split Bregman techniques," *J. Vis. Commun. Image R.*, Vol. 21, pp. 193-199, 2010.
- [7] Ming Jiang and Ge Wang, "Development of blind image deconvolution and its applications," *Journal of X-Ray Science and Technology*, Vol. 11, pp. 13-19, 2003.
- [8] Soong-Der Chen, Abd. Rahman Ramli, "Preserving brightness in histogram equalization based contrast enhancement techniques," *Digital Signal Processing*, Vol. 14, pp. 413-428, 2004.
- [9] A. Papadopoulos, D.I. Fotiadis, L. Costaridou, "Improvement of microcalcification cluster detection in mammography utilizing image enhancement techniques," *Computers in Biology and Medicine*, Vol. 38, pp. 1045 – 1055, 2008.
- [10] Pierre Gravel, Gilles Beaudoin, Jacques A. De Guise, "A Method for Modeling Noise in Medical Images," *IEEE Transactions on Medical Imaging*, Vol. 23, pp. 1221-1231, 2004.